Finite-time Adaptive Sliding Mode Control of DC Microgrids with Constant Power Load

Shekoufeh Neisarian, Mohammad Mehdi Arefi, Navid Vafamand
Shiraz University, Shiraz, Iran
{sh.neisarian, arefi, n.vafamand}@shirazu.ac.ir

Mohammad Javadi, Sérgio F. Santos
INESC TEC
Porto, Portugal
{mohammad.javadi, sergio.santos}@inesctec.pt

João P. S. Catalão
FEUP and INESC TEC
Porto, Portugal
catalao@fe.up.pt

2021 IEEE Madrid PowerTech | 978-1-6654-3597-0/21/$31.00 ©2021 IEEE | DOI: 10.1109/PowerTech46648.2021.9495071

***Abstract*—Due to recent advances in power electronic systems, direct current (DC) microgrid (MG) topology is considered as a promising solution to unite pollution-free renewable energy sources and DC loads. This paper investigates the issue of finite-time robust adaptive stability and tracking issue of a nonlinear direct current (DC) microgrid (MG) comprising a buck converter, linear resistive loads, and nonlinear constant power loads (CPLs). The developed approach is based on a sliding mode controller (SMC) and a nonlinear and nonsingular sliding surface. It is proved that the tracking error converges to zero in a finite-time in the presence of matched disturbance input and uncertainties. The novel controller manipulates the buck converter of the source side to regulate the DC bus voltage by counteracting the destabilizing effect of CPLs and disturbances. Further, the finite value of the convergence time is presented and the effects of the SMC parameter on the stability and transient performance are evaluated. Lastly, numerical simulations are conducted to illustrate the merits of the developed control approach in the viewpoints of fast reference tracking and robust stability.**

***Keywords*—Microgrid, Buck converter, Constant power load, Nonlinear sliding surface, Stability.**

I. INTRODUCTION

Rapid improvements in the technology and production of direct current-direct current (DC-DC) converters, make them a widespread, cost-effective, and high-efficient tool to incorporate distributed renewable energy sources and loads in intergraded power DC microgrid systems. Though, the integration of DC microgrids possesses some key issues, which we should deal with. For example, DC-DC boost converters can behave as a bilinear and non-minimum phase element, which is hard to be controlled. This issue is more challenging when the overall system is subjected to uncertainties and/or disturbances. Moreover, the constant power loads (CPLs) act nonlinear with destabilizing effects. In recent years, several control strategies are presented to regulate buck converters and stabilize microgrids feeding CPLs.

Pioneer works are commonly established in a local small-signal manner based on linear control theory for the linearized models for buck converters and CPLs [1]. To circumvent the local stability, nonlinear controllers are utilized, such as model predictive control [2], backstepping control [3], [4], fuzzy control [5], and sliding mode control (SMC) [6]–[8], passivity control [9] for buck converters and CPLs.

J.P.S. Catalão acknowledges the support by FEDER funds through COMPETE 2020 and by Portuguese funds through FCT, under POCI-01-0145-FEDER-029803 (02/SAICT/2017).

978-1-6654-3597-0/21/$31.00 ©2021 IEEE

Among the above-mentioned buck converter controllers, the SMC is a well-known method robust against uncertainties, disturbances, and time-varying parameters and references [10]–[12]. Compared with the feedback linearization method, the SMC offers a high index of robustness; and in contrast to conventional predictive control methods, it assures the closed-loop stability and tracking performance in-prior. In [13], an SMC is developed for buck converters to improve disturbance rejection performance. Though, the conventional SMC approaches to regulate the MG bus voltage only provide the asymptotic convergence and tracking issue. On the other hand, finite-time stability is incorporated with the conventional SMC to improve the transient phase [14]. In [15], a finite-time SMC is suggested for DC MG power systems with CPLs. Though, in that approach, the overall system should be homogeneous, which can be hard to be checked and cannot involve all power system dynamics. In [16], the issue of finite-time stability is studied based on nonsingular SMC to stabilize the CPLs. However, the finite-time value is not presented in prior. In [17], the finite-time stability of the observer and fixed-time stability of the controller is assured. In [18], the SMC gains must be selected larger than norm of the disturbances to assure finite-time stability. Though, the large value of the gains makes the controller law to have the chattering issue.

In this paper, a novel finite-time adaptive nonsingular terminal sliding mode controller (NTSMC) is suggested for the DC-DC buck converters which supply linear resistive loads and nonlinear destabilizing CPLs. The developed controller uses a nonlinear sliding surface to assure finite-time stability. The finite convergence time is computed to show the relationship of the nonlinear sliding surface and controller parameters with the finite-time stability. Also, the effect of the disturbance and uncertainties on the controller gain is investigated and showed that the overall controller gain can be smaller than the norm of the disturbance. The proposed approach is applied to a typical DC MG with a buck converter, a linear resistive load, and a CPL. Several scenarios are provided to show the transient performance and robustness index of the suggested method.

This paper is continued as follows: In Section II, the considered DC MG topology and its mathematical modeling are presented. In section III, the suggested nonlinear sliding surface and its stabilizing SMC law are presented and the finite-stability analysis for the tracking error is performed. In Section IV, simulation results are given. Section V ends this paper by evoking some concluding remarks and future perspectives.

II. DC MG WITH BUCK CONVERTER AND CPL

A typical DC MG involves some power generators, storages, and loads. These loads can be resistive or constant power, as shown in Fig. 1. The difference between the resistive loads and CPLs is appearing power electronic load converters. These converters are sharply controlled to keep their output powers constant. This can be done based on the property of the controlled load. The CPLs are commonly integrated into DC MGs at the input point of the load converter by assuming the converters are ideal or consume constant power.

Some typical CPLs are DC/DC converters feeding resistive loads and DC/AC inverters feeding electric motors, as shown in Fig. 2. The DC/AC inverter drives a rotating load electric motor with a one-to-one torque-speed profile. If the motor speed ω is sharply regulated to be constant, by the DC/AC inverter, then the torque T and consequently, the power $P = \omega T$ are kept constant. The simplified electric schematic of the DC MG is shown in Fig. 3.

A CPL is modeled by a current source, whose values are dependent on the power level and instantaneous voltage of the CPLs. The electric schematic of Fig. 3 comprises a DC source, a controllable DC/DC conserver, $\mathcal{J}$ CPLs, and $\mathcal{K}$ RLs. Since the resistive loads R_s for $s = 1, \dots, \mathcal{J}$ and CPLs P_{CPL_s} for $s = 1, \dots, \mathcal{K}$ are in parallel, their equivalent resistive load (i.e. R) and CPL (i.e. P) are computed as follows:

$$R = \left(R_1^{-1} + \cdots + R_{\mathcal{J}}^{-1}\right)^{-1} \tag{1}$$

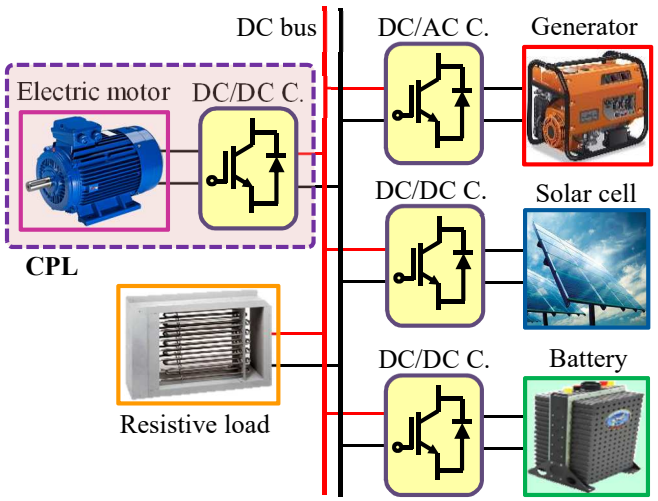

Fig. 1. Power system illustration of an DC MG.

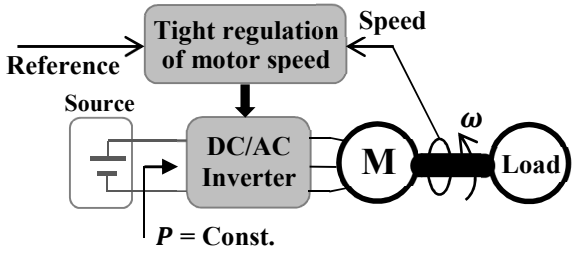

Fig. 2. An example of a CPL.

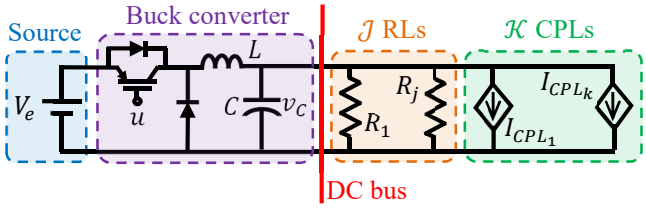

Fig. 3. A basic diagram of the DC MG with $\mathcal{K}$ CPLs and $\mathcal{J}$ resistive loads.

$$P = P_{CPL_1} + \cdots + P_{CPL_{\mathcal{K}}} \tag{2}$$

The DC/DC buck converter is described by an averaged-model and by the duty cycle $u \in \{0,1\}$. The dynamical state-space of the DC MG in Fig. 2. is obtained based on Kirchhoff's current and voltage laws as follows:

$$\begin{cases} L\dfrac{di_L}{dt} = uV_e - v_C \\ C\dfrac{dv_C}{dt} = i_L - \dfrac{v_C}{R} - \dfrac{P}{v_C} \end{cases} \tag{3}$$

where C and L stand for the capacitance and inductance of the buck converter, respectively, i_L and v_c are the inductor current and capacitor voltage, respectively, V_e is the source voltage.

Inspired from [19], the voltage and current errors for the DC MG (3) are as follows:

$$\begin{cases} e_{x_1} = v_c - V_{ref} \\ e_{x_2} = \dot{e}_{x_1} = \dot{v}_c - \dot{V}_{ref} = \dot{v}_c \end{cases} \tag{4}$$

where V_{ref} is the desired reference value of the DC bus voltage. Based on (4), the following state-space error dynamic representation is obtained:

$$\begin{cases} \dot{e}_{x_1} = e_{x_2} \\ \dot{e}_{x_2} = \frac{1}{LC}\left(V_e u - V_{ref} - e_{x_1} + \frac{PLe_{x_2}}{(e_{x_1}+V_{ref})^2}\right) \\ \qquad\qquad - \frac{e_{x_2}}{RC} + d(t,x) \end{cases} \tag{5}$$

where $d(t,x)$ stands for all matched disturbance inputs and uncertainties and x denotes the system states as $x = [x_1, x_2]^T$, where $x_1 = v_c$, $x_2 = \dot{v}_c$.

The matched disturbances and uncertainties $d(t,x)$ are bounded by a polynomial function of the system states with unknown constant coefficients, as follows:

$$|d(t,x)| \le \sum_{k=0}^{r} b_k |x_1|^k + \sum_{m=1}^{r} c_m |x_2|^m \tag{6}$$

The goal is to design an SMC controller that forces the system to track V_{ref} or equivalently, assure the finite-time convergence of the system states of (5) to zero.

III. NONLINEAR SMC AND FINITE-TIME STABILITY ANALYSIS

This section consists of three subsections. Firstly, some basic mathematical preliminaries are mentioned. Secondly, a nonlinear sliding surface is defined and its finite-time stability analysis is investigated.

Then, an NTSMC with an adaptive controller is designed to estimate the unknown upper bound of the bounded disturbances, in finite-time. Finally, the stability analysis of the tracking dynamics is done under the proposed control scheme.

A. Preliminaries

The definition of finite-time stability and several useful lemmas, which are used in the controller design and stability analysis are presented in the following.

Definition 1 [20]**.** Consider a time-invariant nonlinear system (7) where $f: \Gamma \to \Re^n$ is a continuous vector function and $\Gamma \subseteq \Re^n$ is an open neighborhood around the equilibrium point $x = 0$.

$$\dot{x} = f(x) \; with \; f(0) = 0, \; x \in \Gamma \subseteq \Re^n \tag{7}$$

Assume that the system has a unique solution $x(t,x_0)$, for any arbitrary initial condition $x(0) = x_0$. Then, the zero equilibrium point of the system is locally finite-time stable (LFTS) if both below constraints are fulfilled:

a) It is locally asymptotically stable in the region $\hat{\Gamma}$, where $\hat{\Gamma} \subseteq \Gamma$ is an open neighborhood around the equilibrium point.

b) For any initial condition x_0, there exists a finite convergence time $T(x_0): \hat{\Gamma} \setminus \{0\} \to [0,\infty)$ such that $\lim_{t \to T(x_0)} x(t,x_0) \to 0$ and $x(t,x_0) = 0$ for $t \geq T(x_0)$.

The system (7) is globally finite-time stable (GFTS), if $\Gamma = \Re^n$.

Lemma 1 [20]**.** Consider the nonlinear system (7) owning the equilibrium point $x = 0$ and the initial condition x_0. Its equilibrium point is LFTS, if there exists a continuously differentiable function $V(x) > 0: \Gamma \to \Re^+ \cup \{0\}$ such that the following constraint holds for any unique solution $x(t,x_0)$ of the system:

$$\dot{V}(x) \leq -\rho_1 V^{\rho_2}(x) \tag{8}$$

where, $\rho_1 > 0, 0 < \rho_2 < 1$ are arbitrary real coefficients. The finite convergence time $T(x_0)$ is calculated as follows:

$$T(x_0) \leq \left(\rho_1(1-\rho_2)\right)^{-1} V^{1-\rho_2}(x_0) \tag{9}$$

Lemma 2 [21]**.** Suppose $0 < \hbar < 1$, $a_j, j = 1, \dots, n$ are real scalars. The following inequalities hold:

$$\begin{aligned} \sum_{i=1}^{n} |a_i|^{1+\hbar} &\geq \left(\sum_{i=1}^{n} |a_i|^2\right)^{\frac{1+\hbar}{2}} \\ \sum_{i=1}^{n} |a_i|^{0.5} &\geq \left(\sum_{i=1}^{n} |a_i|\right)^{0.5} \end{aligned} \tag{10}$$

B. Nonlinear Nonsingular Terminal Sliding Surface

For the system (5), the proposed nonlinear terminal sliding surface s is designed as follows:

$$s = e_{x_1} + \left(e_{x_2} Q(e_{x_1})\right)^{\frac{q}{l}} \tag{11}$$

where q and l are arbitrary positive odd coefficients, which satisfy $l < q < 2l$. The $Q(e_{x_1})$ is a positive-valued function and determined as follows:

$$Q(e_{x_1}) = \frac{1}{\beta + \alpha e_{x_1}^{\left(\frac{h}{p} - \frac{l}{q}\right)}} \tag{12}$$

where α and β are two positive coefficients selected by the designer and h and p are arbitrary positive odd numbers, which fulfill $h > p$ and $\frac{h}{p} - \frac{l}{q} > 1$.

Inspired from [22], the sliding mode dynamic of the tracking error system, obtained by $s = \dot{s} = 0$, is GFTS and the tracking errors e_{x_1} and e_{x_2} reach zero in the following finite settling time T_s:

$$T_s \leq \frac{1}{\alpha}\left(\frac{p}{h-p}\right) + \frac{1}{\beta}\left(\frac{q}{q-l}\right) \tag{13}$$

Further, from $s = \dot{s} = 0$, the sliding mode dynamics are:

$$\dot{e}_{x_1} = e_{x_2}, \dot{e}_{x_1} = -\alpha e_{x_1}^{\frac{h}{p}} - \beta e_{x_1}^{\frac{l}{q}} \tag{14}$$

C. Finite-time adaptive NTSM controller design via closed-loop stability analysis

In this part, the control input is designed in the form of (15) in order to bring the tracking errors into the sliding mode dynamic (14) for $s = 0$ in finite-time, despite existing disturbances and uncertainties.

$$u = g^{-1}(-f(x) + u_a + u_b + \dot{x}_{d_2}) \tag{15}$$

where $f(x)$, g, u_a, and u_b are chosen based on (5) and the sliding manifold (11), as follows:

$$f(x) = -\frac{x_2}{RC} - \frac{x_1}{LC}, g = \frac{V_e}{LC} \tag{16}$$

$$\begin{aligned} u_a = \frac{-l}{q}\omega \left(e_{x_2}^{2-\frac{q}{l}} \left(Q(e_{x_1})\right)^{\frac{-q}{l}}\right) sgn(se_{x_2}) \\ - \left(\sum_{k=0}^{r} \hat{b}_k |x_1|^k \right. \\ \left. + \sum_{m=1}^{r} \hat{c}_m |x_2|^m \right) sgn(s) \end{aligned} \tag{17}$$

$$\begin{aligned} u_b = \frac{-l}{q}\left(e_{x_2}^{2-\frac{q}{l}} \left(Q(e_{x_1})\right)^{\frac{-q}{l}}\right) \\ + \alpha e_{x_2}^{2} \left(\frac{h}{p} - \frac{l}{q}\right) e_{x_1}^{\frac{h}{p} - \frac{l}{q} - 1} Q(e_{x_1}) \end{aligned} \tag{18}$$

where $\omega > 0$ is an arbitrary parameter and $\hat{b}_k$ and $\hat{c}_m$ are the estimations of unknown constant coefficients in (6). The adaptation laws for $\hat{b}_k$ and $\hat{c}_m$ are as follows:

$$\begin{aligned} \dot{\hat{b}}_k = \zeta_k |x_1|^k \left(\frac{q}{l} e_{x_2}^{\frac{q}{l}-1}\right) \left(Q(e_{x_1})^{\frac{q}{l}}\right) |s|, \; k \\ = 0, \dots, r \text{ with } \hat{b}_k(0) > 0 \end{aligned} \tag{19}$$

$$\begin{aligned} \dot{\hat{c}}_m = \lambda_m |x_2|^m \left(\frac{q}{l} e_{x_2}^{\frac{q}{l}-1}\right) \left(Q(e_{x_1})^{\frac{q}{l}}\right) |s|, \; m \\ = 1, \dots, r \; with \; \hat{c}_m(0) > 0 \end{aligned} \tag{20}$$

where $\zeta_k > 1, \lambda_m > 1$. Since (19) and (20) are positive functions and inspired from [21], $\hat{c}_m$ and $\hat{b}_k$ are bounded by some positive constants b_k^* and c_m^* such that

$$0 < \hat{c}_m < c_m^*, 0 < \hat{b}_k < b_k^* \tag{21}$$

Without loss of generality, each of the constant values b_k^* and c_m^* are broken into two terms as below:

$$\begin{cases} b_k^* = b_k + \eta_k, \eta_k \geq 0 \\ c_m^* = c_m + \gamma_m, \gamma_m \geq 0 \end{cases} \tag{22}$$

The subsequent theorem, states and proves that the proposed control law (15)-(20) warranties the existence of the sliding mode dynamic $s = 0$ in finite-time.

Theorem 1: Consider the tracking error dynamic system (5) and the sliding surface (11).

By applying control input law (15)-(18) and adaptation laws (19) and (20), the tracking errors of the closed-loop system reach the sliding mode dynamic $s = 0$ in the finite reaching time T_r, obtained as follows:

$$\begin{aligned} T_r \leq \frac{1}{\min(\mathcal{K},\mathcal{M},\mathcal{N})} \Big(|s(0)|^2 + \sum_{k=0}^{r} \left|\hat{b}_k(0) - b_k^*\right|^2 \\ + \sum_{m=1}^{r} |\hat{c}_m(0) - c_m^*|^2)^{0.5} \\ \mathcal{K} \triangleq \omega \left|e_{x_2}\right| \end{aligned} \tag{23}$$

$$\mathcal{M} \triangleq \left(\frac{q}{l} e_{x_2}^{\frac{q}{l}-1}\right)\left(\mathcal{Q}(e_{x_1})^{\frac{q}{l}}\right)(min_k(\zeta_k - 1)|x_1|^k)|s|$$

$$\mathcal{N} \triangleq \left(\frac{q}{l} e_{x_2}^{\frac{q}{l}-1}\right)\left(\mathcal{Q}(e_{x_1})^{\frac{q}{l}}\right)(min_m(\lambda_m - 1)|x_2|^m)|s|$$

Proof: Choose a radially unbounded Lyapunov function candidate, as follows

$$V(s,\tilde{b}_k,\tilde{c}_m) = 0.5(|s|^2 + \sum_{m=1}^{r} |\tilde{c}_m|^2 + \sum_{k=0}^{r} \left|\tilde{b}_k\right|^2) \tag{24}$$

where $\tilde{b}_k = \hat{b}_k - b_k^*$ and $\tilde{c}_m = \hat{c}_m - c_m^*$. The time derivative of sliding surface (11) is computed by substituting $\dot{e}_{x_2}$ from (5) and u from (15) as follows:

$$\begin{aligned} \dot{s} = \left(\frac{q}{l} e_{x_2}^{\frac{q}{l}-1}\right)\left(\mathcal{Q}(e_{x_1})^{\frac{q}{l}}\right)\Bigg(d(t,x) \\ - \Bigg(\Bigg(\sum_{k=0}^{r} \hat{b}_k|x_1|^k \\ + \sum_{m=1}^{r} \hat{c}_m|x_2|^m\Bigg) sgn(s)\Bigg)\Bigg) \\ - e_{x_2}\omega sgn(se_{x_2}) \end{aligned} \tag{25}$$

Also, time differentiating the Lyapunov function (24) results in

$$\dot{V}(s,\tilde{b}_k,\tilde{c}_m) = s\dot{s} + \sum_{k=0}^{r} \tilde{b}_k\dot{\hat{b}}_k + \sum_{m=1}^{r} \tilde{c}_m\,\dot{\hat{c}}_m \tag{26}$$

Substituting $\dot{s}$, $\dot{\hat{b}}_k$, and $\dot{\hat{c}}_m$ in (19), (20), and (25), respectively, into (26) obtains

$$\begin{aligned} &\dot{V}(s,\tilde{b}_k,\tilde{c}_m) \\ &= \left(\frac{q}{l} e_{x_2}^{\frac{q}{l}-1}\right)\left(\mathcal{Q}(e_{x_1})^{\frac{q}{l}}\right)\Bigg(s\,d(t,x) \\ &- \Bigg(\Bigg(\sum_{k=0}^{r} \hat{b}_k|x_1|^k + \sum_{m=1}^{r} \hat{c}_m|x_2|^m\Bigg)|s|\Bigg)\Bigg) - \omega|s|\left|e_{x_2}\right| \\ &+ \left(\frac{q}{l} e_{x_2}^{\frac{q}{l}-1}\right)\left(\mathcal{Q}(e_{x_1})^{\frac{q}{l}}\right)|s|\Bigg(\sum_{k=0}^{r} \tilde{b}_k\zeta_k|x_1|^k \\ &+ \sum_{m=1}^{r} \tilde{c}_m\lambda_m|x_2|^m\Bigg) \end{aligned} \tag{27}$$

Since $\left(\frac{q}{l} e_{x_2}^{\frac{q}{l}-1}\right)\left(\mathcal{Q}(e_{x_1})^{\frac{q}{l}}\right)$ is always positive and by considering the definition of $\mathcal{K}$ in (23), the subsequent inequality is achieved:

$$\begin{aligned} &\dot{V}(s,\tilde{b}_k,\tilde{c}_m) \\ &\leq -\mathcal{K}|s| \\ &+ \left(\frac{q}{l} e_{x_2}^{\frac{q}{l}-1}\right)\left(\mathcal{Q}(e_{x_1})^{\frac{q}{l}}\right)|s|\Bigg(|d(t,x)| \\ &- \Bigg(\Bigg(\sum_{k=0}^{r} \hat{b}_k|x_1|^k + \sum_{m=1}^{r} \hat{c}_m|x_2|^m\Bigg)\Bigg)\Bigg) \\ &+ \left(\frac{q}{l} e_{x_2}^{\frac{q}{l}-1}\right)\left(\mathcal{Q}(e_{x_1})^{\frac{q}{l}}\right)|s|\Bigg(\sum_{k=0}^{r} \tilde{b}_k\zeta_k|x_1|^k \\ &+ \sum_{m=1}^{r} \tilde{c}_m\lambda_m|x_2|^m\Bigg) \end{aligned} \tag{28}$$

By reminding (6) and (21), one has

$$|d(t,x)| \leq \sum_{k=0}^{r} b_k^*|x_1|^k + \sum_{m=1}^{r} c_m^*|x_2|^m \tag{29}$$

By applying (29) to (28) and utilizing the definitions $\tilde{b}_k = \hat{b}_k - b_k^*$ and $\tilde{c}_m = \hat{c}_m - c_m^*$ in (22), (28) results that

$$\begin{aligned} &\dot{V}(s,\tilde{b}_k,\tilde{c}_m) \\ &\leq -\mathcal{K}|s| - \left(\frac{q}{l} e_{x_2}^{\frac{q}{l}-1}\right)\left(\mathcal{Q}(e_{x_1})^{\frac{q}{l}}\right)|s|\Big(\sum_{k=0}^{r} \tilde{b}_k|x_1|^k \\ &+ \sum_{m=1}^{r} \tilde{c}_m|x_2|^m\Big) \\ &+ \left(\frac{q}{l} e_{x_2}^{\frac{q}{l}-1}\right)\left(\mathcal{Q}(e_{x_1})^{\frac{q}{l}}\right)|s|\Bigg(\sum_{k=0}^{r} \tilde{b}_k\zeta_k|x_1|^k \\ &+ \sum_{m=1}^{r} \tilde{c}_m\lambda_m|x_2|^m\Bigg) \end{aligned} \tag{30}$$

Since $\tilde{b}_k$ and $\tilde{c}_m$ are always negative, (30) conveniently turns into

$$\dot{V}(s,\tilde{b}_k,\tilde{c}_m) \leq -\mathcal{K}|s| - (\frac{q}{l}e_{x_2}^{\frac{q}{l}-1})\left(\mathcal{Q}(e_{x_1})^{\frac{q}{l}}\right)|s|\left(\sum_{k=0}^{r}|\tilde{b}_k|(\zeta_k-1)|x_1|^k + \sum_{m=1}^{r}|\tilde{c}_m|(\lambda_m-1)|x_2|^m\right) \quad (31)$$

According to the descriptions of $\mathcal{M}$ and $\mathcal{N}$ in (23), (31) is simplified as follows:

$$\dot{V}(s,\tilde{b}_k,\tilde{c}_m) \leq -\mathcal{K}|s| - \mathcal{M}\sum_{k=0}^{r}|\tilde{b}_k| - \mathcal{N}\sum_{m=1}^{r}|\tilde{c}_m| \quad (32)$$

Thereby,

$$\dot{V}(s,\tilde{b}_k,\tilde{c}_m) \leq -\sqrt{2}(\min(\mathcal{K},\mathcal{M},\mathcal{N}))(\frac{1}{\sqrt{2}}|s| + \frac{1}{\sqrt{2}}\sum_{k=0}^{r}|\tilde{b}_k| + \frac{1}{\sqrt{2}}\sum_{m=1}^{r}|\tilde{c}_m|) \quad (33)$$

Consequently, defining $\mathscr{b} \triangleq \min(\mathcal{K},\mathcal{M},\mathcal{N})$, one concludes $\dot{V} \leq -\sqrt{2}\,\mathscr{b}V^{\frac{1}{2}}$. Thereby, the finite-time stability is satisfied. As a result, referring to Lemma 1 and choosing $\rho_1 = \sqrt{2}\,\mathscr{b}$ and $\rho_2 = \frac{1}{2}$, one can conclude that s converges zero in finite-time T_r (23) and the existence of the sliding mode dynamic $s = 0$ is guaranteed. Therefore, the proof is completed. ■

Remark 1: The proposed control scheme in this paper can satisfy the described control objective (finite-time tracking problem) in finite time $T_{total} = T_r + T_s$. The finite time T_r and T_s are determined by (23) and (13).

IV. Numerical Simulation Results

In this part, numerical simulations are considered to show the advantages of the proposed approach in viewpoints of fast-tracking performance and highly robust stability.

The parameters' nominal values and their uncertainty percentage for the DC MG as well as the controller parameters are given in Table I. Further, the external disturbance is chosen as $d(t,x) = 0.5 + 0.1x_1 + 0.1x_2$ and the desired output reference is $V_{ref} = 240\ [V]$.

The proposed approach is compared with the [9], in which a disturbance observer-based passivity controller is suggested. Fig. 4 depicts the DC MG bus voltage, the duty cycle control input, and the sliding surface of the controller.

As can be seen in Fig. 4, both approaches offer an accurate voltage tracking. Though, the proposed approach provides a faster transient performance than [9]. The evolution of the upper bounds of the disturbance input, i.e. $\hat{b}_0$, $\hat{b}_1$, and $\hat{c}_0$ are given in Fig. 5. One observes that the term $\hat{c}_0$, which is related to the x_2 converges very fast and the other terms reaches to their steady-state values about 0.7 seconds.

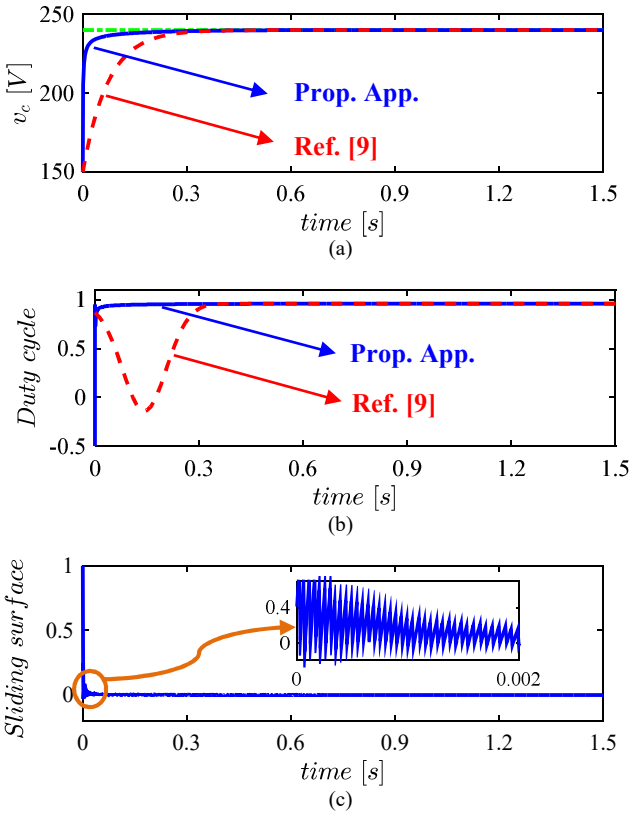

Fig. 4. Closed-loop system output, input, and sliding surface.

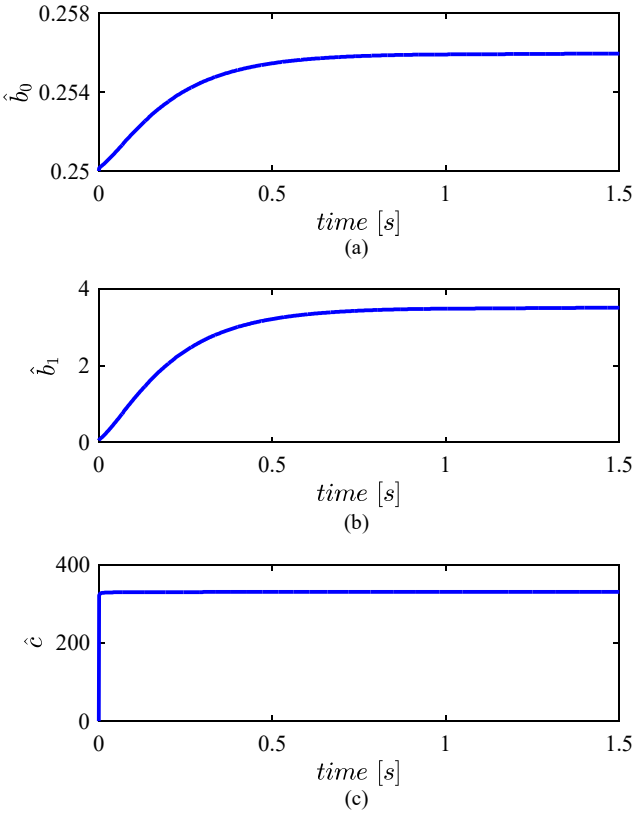

Fig. 5. Adaptive parameters of disturbance input upper bounds.

TABLE I. SYSTEM AND CONTROL PARAMETER VALUES.

Power system uncertain parameters			
Parameter	Value	Parameter	Value
P	$300 \pm 10\%$	C	$5 \times 10^{-4} \pm 15\%$
R	$30 \pm 20\%$	L	$3 \times 10^{-3} \pm 15\%$
V_e	$250 \pm 5\%$		
Controller nominal parameters			
Parameter	Value	Parameter	Value
α	0.7	q	11
β	6	ω	7
h	13	ζ_0	20
p	5	ζ_1	50
l	9	λ_1	200

V. CONCLUSION

In this paper, a novel controller for a class of nonlinear DC MGs was proposed. The considered case study islanded DC MGs involved a DC source, source-side buck converter, and linear and nonlinear loads such as CPLs. The buck converter was manipulated to not only stabilize the overall system, but also to neglect the effect of external disturbances and uncertainties. To achieve this goal, an improved nonsingular sliding mode controller was suggested. Based on a nonlinear sliding surface, a finite-time stabilizing SMC was developed for the DC MGs. For the tracking error dynamics, the finite-time convergence to zero was demonstrated. Also, the finite convergence time was computed as a function of the initial conditions and the parameters of the SMC. Numerical simulations showed the advantages of the robust adaptive controller. It was revealed that the DC bus voltage reached its desired reference in about 0.5 seconds for both the nominal and uncertain DC MG systems. For future work, equipping the SMC controller with a sliding mode observer is suggested to reduce the cost of installing both voltage and current sensors.

REFERENCES

[1] Q. Xu, N. Vafamand, L. Chen, T. Dragicevic, L. Xie, and F. Blaabjerg, "Review on Advanced Control Technologies for Bidirectional DC/DC Converters in DC Microgrids," *IEEE J. Emerg. Sel. Top. Power Electron.*, pp. 1–1, 2020, doi: 10.1109/JESTPE.2020.2978064.

[2] N. Vafamand, S. Yousefizadeh, M. H. Khooban, J. D. Bendtsen, and T. Dragicevic, "Adaptive TS Fuzzy-Based MPC for DC Microgrids With Dynamic CPLs: Nonlinear Power Observer Approach," *IEEE Syst. J.*, vol. 13, no. 3, pp. 3203–3210, 2018, doi: 10.1109/JSYST.2018.2880135.

[3] S. Yousefizadeh, J. D. Bendtsen, N. Vafamand, M. H. Khooban, T. Dragicevic, and F. Blaabjerg, "Tracking Control for a DC Microgrid Feeding Uncertain Loads in More Electric Aircraft: Adaptive Backstepping Approach," *IEEE Trans. Ind. Electron.*, 2018.

[4] T. K. Nizami, A. Chakravarty, and C. Mahanta, "Analysis and experimental investigation into a finite time current observer based adaptive backstepping control of buck converters," *J. Frankl. Inst.*, vol. 355, no. 12, pp. 4996–5017, Aug. 2018, doi: 10.1016/j.jfranklin.2018.05.026.

[5] N. Vafamand, M. H. Khooban, T. Dragicevic, F. Blaabjerg, and J. Boudjadar, "Robust Non-Fragile Fuzzy Control of Uncertain DC Microgrids Feeding Constant Power Loads," *IEEE Trans. Power Electron.*, vol. 34, no. 11, pp. 11300–11308, Nov. 2019, doi: 10.1109/TPEL.2019.2896019.

[6] M. Zhang, Y. Li, F. Liu, L. Luo, Y. Cao, and M. Shahidehpour, "Voltage stability analysis and sliding-mode control method for rectifier in DC systems with constant power loads," *IEEE J. Emerg. Sel. Top. Power Electron.*, vol. 5, no. 4, pp. 1621–1630, 2017, doi: 10.1109/JESTPE.2017.2723482.

[7] A. El Aroudi, B. A. Mart\'\inez-Treviño, E. Vidal-Idiarte, and A. Cid-Pastor, "Fixed Switching Frequency Digital Sliding-Mode Control of DC-DC Power Supplies Loaded by Constant Power Loads with Inrush Current Limitation Capability," *Energies*, vol. 12, no. 6, p. 1055, 2019.

[8] Z. Wang, S. Li, and Q. Li, "Discrete-Time Fast Terminal Sliding Mode Control Design for DC–DC Buck Converters With Mismatched Disturbances," *IEEE Trans. Ind. Inform.*, vol. 16, no. 2, pp. 1204–1213, Feb. 2020, doi: 10.1109/TII.2019.2937878.

[9] M. A. Hassan, E. Li, X. Li, T. Li, C. Duan, and S. Chi, "Adaptive Passivity-Based Control of dc–dc Buck Power Converter With Constant Power Load in DC Microgrid Systems," *IEEE J. Emerg. Sel. Top. Power Electron.*, vol. 7, no. 3, pp. 2029–2040, Sep. 2019, doi: 10.1109/JESTPE.2018.2874449.

[10] A. Rastegari, M. M. Arefi, and M. H. Asemani, "Robust H∞ sliding mode observer-based fault-tolerant control for One-sided Lipschitz nonlinear systems," *Asian J. Control*, vol. 21, no. 1, pp. 114–129, Jan. 2019, doi: 10.1002/asjc.2062.

[11] A. Abooee, M. Hayeri Mehrizi, M. M. Arefi, and S. Yin, "Finite-time sliding mode control for a 3-DOF fully actuated autonomous surface vehicle," *Trans. Inst. Meas. Control*, vol. 43, no. 2, pp. 371–389, Jan. 2021, doi: 10.1177/0142331220957516.

[12] M. M. Mardani, N. Vafamand, M. Shokrian Zeini, M. Shasadeghi, and A. Khayatian, "Sum-of-Squares-Based Finite-Time Adaptive Sliding Mode Control of Uncertain Polynomial Systems With Input Nonlinearities," *Asian J. Control*, vol. 20, no. 4, pp. 1658–1662, 2018, doi: 10.1002/asjc.1625.

[13] B. Wang, G. Ma, D. Xu, L. Zhang, and J. Zhou, "Switching sliding-mode control strategy based on multi-type restrictive condition for voltage control of buck converter in auxiliary energy source," *Appl. Energy*, vol. 228, pp. 1373–1384, Oct. 2018, doi: 10.1016/j.apenergy.2018.06.141.

[14] Q. Xu, C. Zhang, Z. Xu, P. Lin, and P. Wang, "A Composite Finite-Time Controller for Decentralized Power Sharing and Stabilization of Hybrid Fuel Cell/Supercapacitor System With Constant Power Load," *IEEE Trans. Ind. Electron.*, vol. 68, no. 2, pp. 1388–1400, Feb. 2021, doi: 10.1109/TIE.2020.2967660.

[15] P. Lin, C. Zhang, X. Zhang, H. Iu, Y. Yang, and F. Blaabjerg, "Finite-Time Large Signal Stabilization for High Power DC Microgrids with Exact Offsetting of Destabilizing Effects," *IEEE Trans. Ind. Electron.*, pp. 1–1, 2020, doi: 10.1109/TIE.2020.2987275.

[16] Z. Wang, S. Li, and Q. Li, "Continuous Nonsingular Terminal Sliding Mode Control of DC–DC Boost Converters Subject to Time-Varying Disturbances," *IEEE Trans. Circuits Syst. II Express Briefs*, vol. 67, no. 11, pp. 2552–2556, Nov. 2020, doi: 10.1109/TCSII.2019.2955711.

[17] N. Sarrafan, J. Zarei, R. Razavi-Far, M. Saif, and M.-H. Khooban, "A Novel On-Board DC/DC Converter Controller Feeding Uncertain Constant Power Loads," *IEEE J. Emerg. Sel. Top. Power Electron.*, pp. 1–1, 2020, doi: 10.1109/JESTPE.2019.2963417.

[18] J. Pan, H. Cui, Z. Wang, S. Li, and Q. Li, "Finite-time control for DC-DC boost converter using nonsingular terminal sliding modes via exact feedback linearization," in *2017 36th Chinese Control Conference (CCC)*, Dalian, China, Jul. 2017, pp. 9302–9307, doi: 10.23919/ChiCC.2017.8028839.

[19] H. Komurcugil, "Non-singular terminal sliding-mode control of DC–DC buck converters," *Control Eng. Pract.*, vol. 21, no. 3, pp. 321–332, Mar. 2013, doi: 10.1016/j.conengprac.2012.11.006.

[20] A. Abooee and M. M. Arefi, "Robust Finite-Time Stabilizers for a Connected Chain of Nonlinear Double-Integrator Systems," *IEEE Syst. J.*, vol. 13, no. 1, pp. 833–841, Mar. 2019, doi: 10.1109/JSYST.2018.2851153.

[21] F. Plestan, Y. Shtessel, V. Brégeault, and A. Poznyak, "New methodologies for adaptive sliding mode control," *Int. J. Control*, vol. 83, no. 9, pp. 1907–1919, Sep. 2010, doi: 10.1080/00207179.2010.501385.

[22] Z. Zuo, "Nonsingular fixed-time consensus tracking for second-order multi-agent networks," *Automatica*, vol. 54, pp. 305–309, Apr. 2015, doi: 10.1016/j.automatica.2015.01.021.